Importance of Coulomb correlation on the quantum anomalous Hall effect in V-doped topological insulators

Jeongwoo Kim, Hui Wang, and Ruqian Wu

Phys. Rev. B **97**, 125118 — Published 13 March 2018

DOI: 10.1103/PhysRevB.97.125118

Importance of Coulomb correlation on the quantum anomalous Hall effect in V-doped topological insulators

Jeongwoo Kim, Hui Wang, & Ruqian Wu*

Department of Physics and Astronomy, University of California, Irvine, California 92697-4575, USA

Abstract:

The presence of the quantum anomalous Hall effect (QAHE) in a V-doped topological insulator (TI) has not yet been understood from band structure studies. Here, we demonstrate the importance of including the correlation effect in density functional theory (DFT) calculations, in the format as simple as the Hubbard U, for the determination of the topological properties of these materials. Our results show that the correlation effect turns a V-doped TI thin film to a Mott insulator and facilitate it entering the quantum anomalous Hall phase. Even the ferromagnetic ordering is also strongly affected by the inclusion of the U-term. This work satisfactorily explains recent experimental observations and highlights the essentialness of having the Coulomb correlation effect in DFT studies of magnetic TIs.

Email: wur@uci.edu

PACS numbers: 75.50.Pp, 73.20.At, 73.43.Cd

Ⅰ. INTRODUCTION

Attaining a quantized Hall resistance without using an external magnetic field has been pursued for a quite long time,[1-3] ever since the discovery of quantum Hall effect opened an era of topological quantum phenomena.[4] To this end, the topologically distinct state with an integer Chern number, so called the quantum anomalous Hall effect (QAHE), was predicted in magnetic doped topological insulators (TIs)[5] and successfully realized in Cr- or V-doped $(Bi,Sb)_2Te_3$ (BST).[6-10] The strong interplay between the long-range ferromagnetic ordering of magnetic dopants and the nontrivial band topology attributed to the large spin-orbit coupling (SOC) of TIs gives rise to the chiral edge state along with the vanished longitudinal conductivity.[11-13] These properties are very promising for the design of various innovative spintronic devices that require high energy efficiency, rapid information processing, and stable quantum coherence in operations. As continuous endeavors have been dedicated to increase the characteristic temperature of QAHE, it is interesting to note that V-doped BST exhibits a larger coercive field and higher Curie temperature than Cr-doped BST at the same doping concentration.[10] In addition, the QAHE was observed at a higher temperature (~130 mK) in V-doped BST[10] in comparison to ~30 mK in Cr-doped BST.[6] This was a surprise since V-doped TIs were not classified as a good platform to host the QAHE because the insulating ferromagnetic (FM) state, one of the prerequisites for the realization of QAHE, was absent according to first-principles calculations.[5, 14, 15] In addition, the predicted *d*-bands near the Fermi level were not found in experiments, and the longitudinal conduction was hence unexpectedly suppressed.[10, 16-18] Obviously, it is indispensable to investigate the unexplored factors responsible for the discrepancies and to find ways for achieving QAHE at even higher temperature.

One possible explanation for the disparity between theory and experiment is the

Anderson localization of *d*-orbitals of V, which was neglected in previous theoretical studies.[5] However, obvious signatures of a quantum phase transition from a quantum anomalous Hall insulator to an Anderson insulator refute the possibility of the coexistence of the QAHE and Anderson localization.[19] Another possibility is a Mott insulator transition driven by the strong correlation effect of *d*-orbitals of dopants. Nevertheless, the correlation effect on the electronic structure and its band topology has not been carefully examined so far. This inspires us to explore the mysterious disappearance of impurity bands around the Fermi level and the association between the correlation effect and the topological features in V-doped TI.

In this work, we investigate how the correlation effect affects the ferromagnetic ordering and band topology in V-doped Sb_2Te_3 using density functional theory (DFT) calculations. We show that the ferromagnetic order is determined by two separable factors, the *p*-orbital-assisted long-range superexchange interaction and the short-range double exchange interaction. With a systematic examination for the progressive change of the electronic structure of $(Sb,V)_2Te_3$ upon increasing the correlation and SOC, we demonstrate that the on-site Coulomb interaction plays an important role in determining the magnetic and topological properties of V-doped TIs. Our results not only provide useful clues for the understanding of the recondite physics involved in the realization of QAHE in V-doped TIs, but also show the possibility of coexistence of different quantum phenomena in a single material.

Ⅱ. METHOD

We carry out DFT calculations using the projected augmented plane-wave method[20, 21] as implemented in the Vienna *ab initio* simulation package (VASP).[22] The Perdew-Burke-Ernzerhof functional of the generalized gradient approximation (GGA) is used for the

description of exchange-correlation interactions among electrons,[23] along with the van der Waals corrections that are needed to describe the interaction between adjacent quintuple layers (QLs) of TIs.[24] SOC is included in the self-consistent loop. The energy cutoff for the plane-wave-basis expansion is chosen to be 300 eV. We adopt the GGA +*U* scheme to consider the correlation effect on the *d*-shell of V atoms.[15, 25] We note that the topology of 3*d* magnetic system has been successfully described by the static correlation effect without the consideration of the dynamic correlation effect.[26, 27] A (4×4) hexagonal supercell expanded along the (111) plane with 3 QLs along the *z*-axis (240 atoms/supercell) is used to calculate the electronic structure and exchange energy of a bulk model for V-doped Sb_2Te_3. The model for the surface of TI consists of a 4-QL slab which expands into a (3×3) supercell in the lateral plane and is separated by a 15 Å vacuum along the surface normal (180 atoms/supercell). We employ 4×4×1 ***k***-point grid to sample the Brillouin zone. The atomic positions are fully relaxed until the convergence of total energies becomes better than 0.1 meV. In this study, we only consider configurations with V atoms substituting on the Sb sites, which are energetically more stable.[14] To describe the topological nature, the Chern numbers are calculated from the Berry curvature, $\Omega(\mathbf{k})$, which is defined as,[28, 29]

$$\Omega(\mathbf{k}) = -2\,\mathrm{Im}\sum_{n}\sum_{n'\neq n} f_n \frac{\langle\psi_{n\mathbf{k}}|v_x|\psi_{n'\mathbf{k}}\rangle\langle\psi_{n'\mathbf{k}}|v_y|\psi_{n\mathbf{k}}\rangle}{(\varepsilon_{n'\mathbf{k}}-\varepsilon_{n\mathbf{k}})^2},$$

where n is the band index, f_n is the Fermi-Dirac distribution function, $v_{x(y)}$ is the velocity operator, $\psi_{n\mathbf{k}}$ and $\varepsilon_{n\mathbf{k}}$ are the Bloch wave-function and eigenenergy of the n-th band at a **k**-point, respectively. The Berry curvature and the surface spectral weight of semi-infinite slabs are also estimated from a tight-binding Hamiltonian constructed by the maximally-localized Wannier functions using the WANNIER90 package.[30, 31]

Ⅲ. RESULT AND DISCUSSIONS

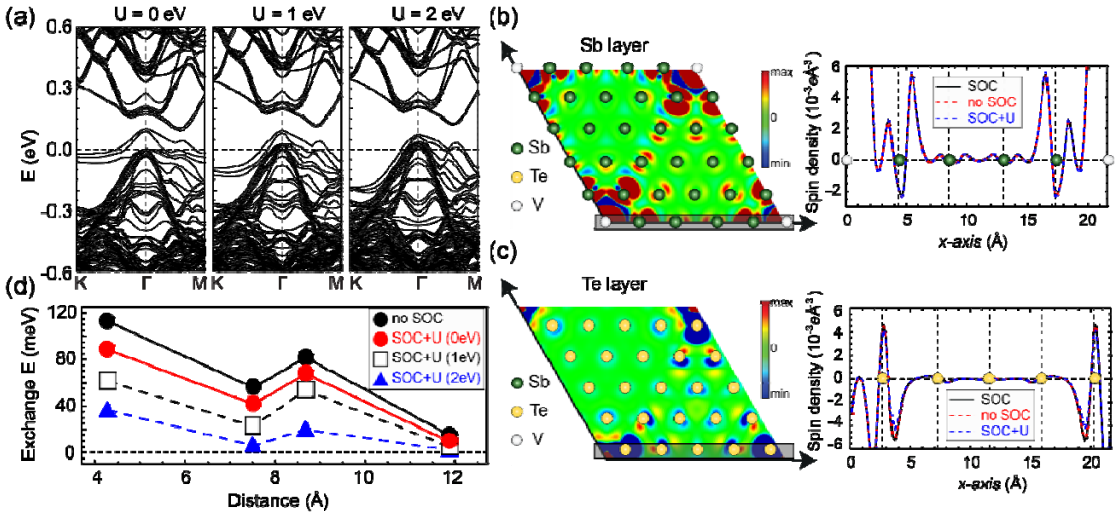

Figure 1 (a) Calculated band structures of V-doped (1.0 %) Sb_2Te_3 with different U values. (b) The spin density of V-doped Sb_2Te_3 (U=0) in the Sb layer with V dopants (left panel) and its line profile corresponding to the shaded regions of Sb layer (right panel), respectively. (c) The spin density of V-doped Sb_2Te_3 (U=0) in the Te layer with V dopants (left panel) and its line profile corresponding to the shaded regions of Te layer (right panel), respectively. The color scale covers the range from -4.0×10^{-4} to 4.0×10^{-4} e/Å^3. For the SOC+U case, the U value is set to 1 eV. (d) Exchange energies as a function of V-V distance for Sb_2Te_3. Positive (negative) values imply ferromagnetic and antiferromagnetic alignments, respectively.

We first investigate how the electronic structure of the bulk Sb_2Te_3 is modified by V doping. As already reported,[5, 14, 15] the emergence of partially occupied *d*-orbitals near the Fermi level for U=0 renders V-doped (1.0%) Sb_2Te_3 metallic [Fig. 1(a)]. Since the bulk conduction is successfully restrained in V-doped TIs,[10, 18] we examine the possibility of opening a band gap by adding the correlation effect on the *d*-orbitals of V. Interestingly, as we increase the on-site Coulomb energy, U, the *d*-bands originating from V atoms move downward and the band gap of the bulk Sb_2Te_3 is restored. With the inclusion of U, the band gap opening still holds in a higher V concentration (Fig. S1).[32] For U=1 eV, the calculated magnetic moment (2.2 μ_B) is also comparable to the experimentally estimated value (1.5

μ_B).[10] The recovery of the insulating nature, a crucial prerequisite for the QAHE, implies that the correlation effect should be considered for an appropriate description of the V-doped TIs.

To understand the ferromagnetic ordering between V dopants in Sb_2Te_3, the spin density of $(Sb,V)_2Te_3$ is given in Figs. 1(b) and(c). As was also found in $(Sb,Cr)_2Te_3$,[33] the induced spin density around the cation sites is positive, *i.e.*, parallel to the spin of V; whereas it becomes negative around the anion sites. The magnetic property is also insensitive to the SOC effect and the correlation effect in V-doped Sb_2Te_3 when V dopants are separated more than 20 Å [Figs. 1(b) and(c)]. This suggests that the localized spin states are mediated by a long-range network of *p*-orbitals of anions, as was observed in Cr-doped TIs.[33] Furthermore, the partially filled *d*-bands in $(Sb,V)_2Te_3$ also provide a short-range double exchange channel for magnetic ordering. This term is very sensitive to the electronic structure near the Fermi level. For example, the energy difference between the parallel and antiparallel spin configurations (*i.e.*, the exchange energy) increases if SOC is not considered in our calculations (black solid line), and decreases with increasing U values (dashed lines) [Fig. 1(d)]. This is understandable since the double exchange contribution decreases as *d*-bands are pushed away from the Fermi level.

To investigate the correlation effect on the topological surface states (TSSs) of magnetic TIs and disentangle the major factors for the observation of QAHE, we calculate the band structure of V-doped TI films. To be comparable with experiments,[10] the thickness of TI thin films is chosen to be 4 QLs (Note that we also tested 5-QL V-doped Sb_2Te_3 films and found no substantial difference as seen in Fig. S2).[32] V dopants are placed on the cation sites only in the outermost QL, where the TSSs weight is the largest (see Fig. S3 for the different configurations).[32, 34] The effective doping concentration in the topmost QL is 5.6 %, very close to what was used in experiment for the realization of QAHE.[10] We found that the

characteristic electronic structure of $(Sb,V)_2Te_3$ is well maintained even at a higher doping level (Fig. S4).[32] Moreover, the electronic structures of $(Bi,Sb)_2Te_3$ and Sb_2Te_3 are very similar under the same V doping (2.8 %) [Fig. 2(a)], suggesting that Bi codoping (13.9 %) does not cause drastic changes in bands. Hereafter, we focus on results for V-doped Sb_2Te_3 (2.8 %) for the discussion of fundamental physics of V-doping-induced QAHE.

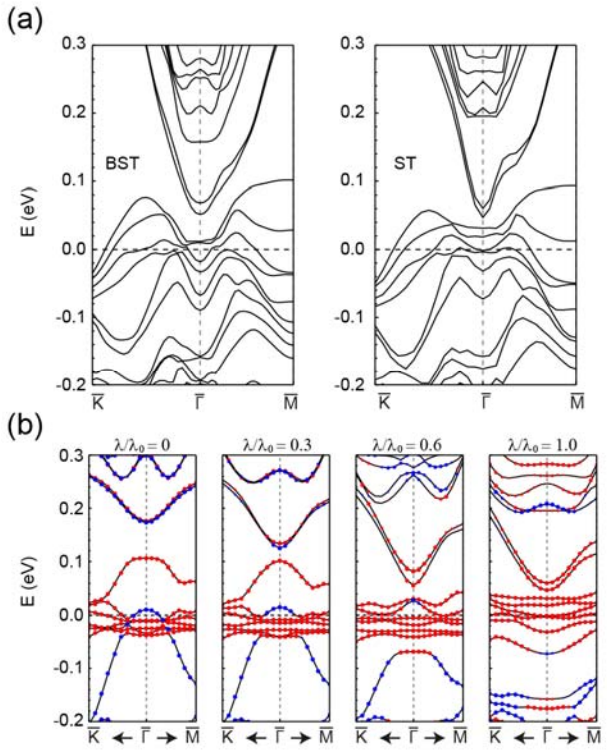

Figure 2 (a) Calculated band structures of V-doped (2.8 %) $(Bi,Sb)_2Te_3$ and Sb_2Te_3 in a 4QL-slab geometry without the U effect. (b) Calculated band structures of 4-QL V-doped Sb_2Te_3 without the U effect for varying SOC of V with respect to its native strength. V dopants are placed in the outermost QL. Spin up (down) states are marked by red (blue) dots.

By adjusting the SOC strength, we tracked progressive changes in the band structure of V-doped Sb_2Te_3 without *U* effect [Fig. 2(b)]. When we turn off the SOC (λ/λ_0=0), the conduction bands are almost degenerate around 0.18 eV while the valence bands exhibit a wide spin splitting of 0.1 eV at the Γ point. As we increase the SOC strength (λ/λ_0=0.3), the

conduction and valence bands become closer to each other and the conduction bands start to be magnetized. When the SOC strength reaches 60 % of its native value (λ/λ_0=0.6), conduction bands around 0.05 eV have the same spin polarization, and band inversion between two spins occurs around the Γ-point. For the valence bands, a clear identification of TSSs is not made due to the strong overlap between the flat *d*-orbitals and the TSSs around the Fermi level. This band topology is maintained as we further increase SOC strength to λ/λ_0=1, in spite of the alternation of band positions. From these results, we found that the nontrivial band order can be attained without considering the correlation effect.

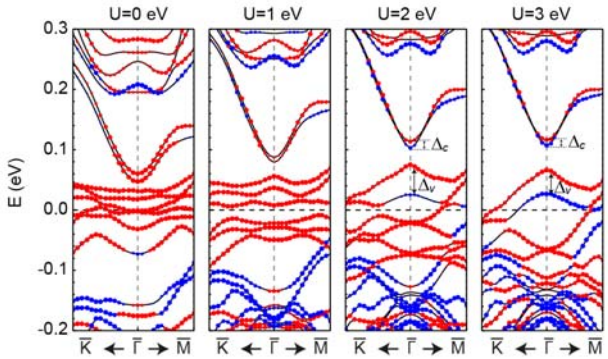

Figure 3 Calculated band structure of 4-QL (2.8 %) V-doped Sb_2Te_3 for varying U values. V dopants are placed in the outermost QL. Spin up (down) states are marked by red (blue) color.

Now we investigate how the *U* effect alters the electronic structure of V-doped (2.8 %) Sb_2Te_3 thin film (Fig. 3). The band inversion, the most essential signature of the nontrivial band topology, occurs at the very narrow area around the Γ point and we zoomed in to that area to see the band evolution more clearly. Because of the *U* effect, the flat *d*-bands of V are pushed away from the Fermi level and the TSSs become sharper. Consequently, the band gap around 0.05 eV is opened at the Γ point by the correlation effect, which is the prototypical characteristic of a Mott insulator. This band structure agrees with recent observation of angle-resolved photoemission spectroscopy,[16, 17] which suggested that the TSS of V-doped TI retains its linear dispersion near the Γ point. Again, this indicates the necessity

of introducing a proper *U* value to correctly describe the electronic structure of V-doped TI thin film. We note that the TI thin film becomes slightly *p*-doped due to the shift of the *d*-orbitals in our calculations but in experiment the Fermi level can be finely tuned by adjusting the composition ratio of Bi and Sb.[35] In addition, the valence state of V is estimated to be a mixture of 3+ and 4+ (or/and 5+) in experiment as opposed to 3+ of Sb atoms and thus the extra free electrons originating from V dopants are expected to neutralize the *p*-type carriers of TI thin film.[10]

Another intriguing finding is that the band topology of V-doped Sb_2Te_3 can be changed by the magnitude of the *U* value. The two lowest conductions bands around 0.1 eV (or upper Dirac cones) have the same spin at the Γ point if the *U* value is less than 2 eV. This means that the inverted band order is maintained. As the *U* value increases further, the conduction bands turn out to have two different spin states and their energy splitting (Δ_c) decreases. The alteration of the band topology can be attributed to the diminished exchange splitting of the TSSs due to the weakening of hybridization between the TSS and the *d*-orbitals of V. The effective exchange field exerted on the TSS decreases as the *d*-bands of V are shifted away from the Fermi level by the correlation effect (Fig. 4). As a result of the shift of *d* orbitals, the hybridization between the TSS and the *d* orbitals becomes weak and thus the exchange field that the TSSs experience can be varied. Quantitatively, the valence band splitting (Δ_v) reduces from 49.5 to 39.3meV as we increase *U* value from 2 to 3 eV. Clearly, the spin polarization of TSS is influenced by the degree of hybridization between TSS and *d*-bands of magnetic impurities. Therefore, considering the nontrivial band topology for the QAHE and the sharp band dispersion of experiment, the optimum *U* value should be in the range of 1 to 2 eV. We note that the optimum U value determined by the comparison with the experimental results[10, 16] is quite different from the value used in VO_2 or $SrVO_3$ since it is

material dependent[15, 25, 36-38].

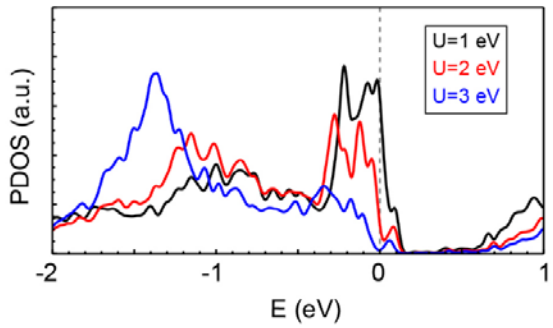

Figure 4. Density of states of V d orbitals for varying the U value from 1 to 3 eV in 4-QL (2.8 %) V-doped Sb_2Te_3.

To elucidate the relation between the QAHE and the correlation effect in V-doped TIs, we carry out Berry curvature calculations and determine the Chern numbers for varying *U* values. We use a (2×2) supercell possible for the Berry curvature calculation to circumvent the enormous computational cost of the large supercell. The underlying physics of $(Sb,V)_2Te_3$ is still adequately captured in the smaller supercell with 6.3 % of V concentration (Fig. 5). As we increase the *U* value, the TSSs with a liner dispersion (around the Dirac point) are identified more clearly. Until the *U* value reach 1 eV, trivial metallic states are lying at the same energy range as the TSSs. If the Fermi level is pinned to the Dirac point (dashed line) by changing the composition ratio, the insulating state is obtained at 2 eV of *U* value. Above that (*U*=3 eV), the shoulder peak observed along the Γ-M direction become lower than TSSs. Therefore, the gap opening around the Dirac point by the inclusion of the correlation effect indicates that V-doped Sb_2Te_3 is a Mott insulator when the Fermi level is appropriately tuned.

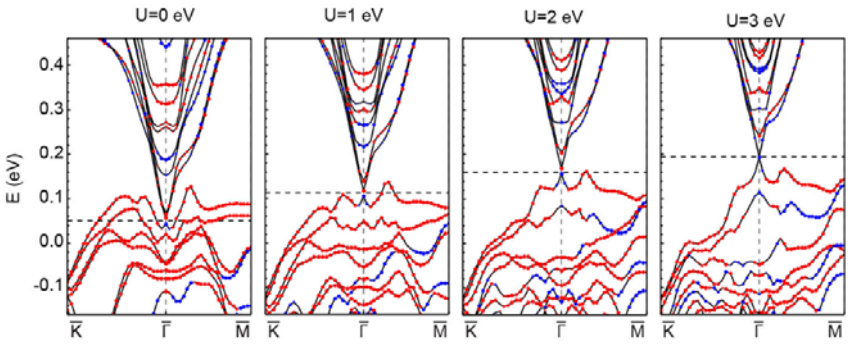

Figure 5. Calculated band structure of 4-QL (6.3 %) V-doped Sb_2Te_3 for varying the U value. V dopants are located at the outermost QL. The U value of V atom is indicated at the top of the panels. Spin up (down) states are marked by red (blue) dots. Dashed lines are set to the Dirac point of V-doped Sb_2Te_3 thin films.

Figure 6 (a) shows that the anomalous Hall conductivity at the Dirac point is close to 1 as long as the *U* value is smaller than 2 eV, which means that the QAHE is achieved by V doping in the Sb_2Te_3 thin film. We note that, due to the intervention of trivial metallic states (Fig. 5), the anomalous Hall conductivity deviates from an integer value. The nontrivial topology of the higher doping (Fig. 4) appears to persist up to higher *U* values in comparison with the lower doping case (Fig. 3). From our results, we can infer that the QAHE is established in a wide range of *U* value and, given that *U*=2 eV is a common choice,[25] the QAHE is expected to occur readily in V-doped TIs. The spin polarized band structure of Figure 5 shows that the linear dispersion of TSS is well preserved and two spin states are inverted when *U*=2 eV is applied. The quantized Hall conductivity [Fig. 6(b)] and the existence of the edge states connecting valence and conduction bands near the Dirac point in a semi-infinite boundary [Fig. 6(c)] are another convincing evidence for the QAHE in V-doped TI thin film with the correlation effect.

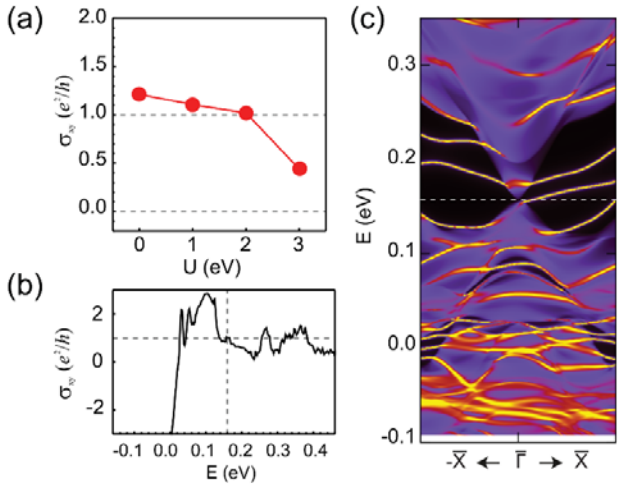

Figure 6 (a) The variation of the anomalous Hall conductivity (σ_{xy}) upon different U value of V atom in 4-QL V-doped (6.3 %) Sb_2Te_3. (b) Calculated anomalous Hall conductivity (σ_{xy}) of 4-QL (6.3 %) V-doped Sb_2Te_3 with the U effect (2 eV). Horizontal dashed line marks the Hall conductivity with a Chern number of 1. (c) Calculated edge state for the semi-infinite boundary of 4-QL V-doped Sb_2Te_3. Vertical dashed line in (b) and horizontal dashed line in (c) are set to the Dirac point.

Ⅳ. SUMMARY

In summary, we demonstrate that the correlation effect is a crucial factor for the manifestation of the QAHE in V-doped TIs. We show that the ferromagnetic ordering of $(Sb,V)_2Te_3$ is further enhanced by the double exchange interaction between the partially filled *d*-bands relative to that in Cr-doped Sb_2Te_3. V-doped TI thin film turns into a Mott insulator by the introduction of the on-site Coulomb energy and it gives rise to the QAHE in combination with the nontrivial-band order. Our studies unravel the mysterious disagreement between experiment and theory, and furthermore provides a perfect example showing the coexistence of two distinct quantum phenomena, the correlation-driven-Mott insulator and the topology-driven QAHE.

This work was support by the SHINES, an Energy Frontier Research Center founded by the U. S. Department of Energy, Office of Science, Basic Energy Science under Award SC0012670. Calculations were performed on parallel computers at NERSC supercomputer centers.

References

[1] F. D. M. Haldane, Phys. Rev. Lett. **61**, 2015 (1988).
[2] M. Onoda and N. Nagaosa, Phys. Rev. Lett. **90**, 206601 (2003).
[3] C.-X. Liu, X.-L. Qi, X. Dai, Z. Fang, and S.-C. Zhang, Phys. Rev. Lett. **101**, 146802 (2008).
[4] K. v. Klitzing, G. Dorda, and M. Pepper, Phys. Rev. Lett. **45**, 494 (1980).
[5] R. Yu, W. Zhang, H.-J. Zhang, S.-C. Zhang, X. Dai, and Z. Fang, Science **329**, 61 (2010).
[6] C.-Z. Chang, et al., Science **340**, 167 (2013).
[7] J. G. Checkelsky, R. Yoshimi, A. Tsukazaki, K. S. Takahashi, Y. Kozuka, J. Falson, M. Kawasaki, and Y. Tokura, Nat. Phys. **10**, 731 (2014).
[8] X. Kou, et al., Phys. Rev. Lett. **113**, 137201 (2014).
[9] A. J. Bestwick, E. J. Fox, X. Kou, L. Pan, K. L. Wang, and D. Goldhaber-Gordon, Phys. Rev. Lett. **114**, 187201 (2015).
[10] C.-Z. Chang, et al., Nat. Mater. **14**, 473 (2015).
[11] H. Jiang, Z. Qiao, H. Liu, and Q. Niu, Phys. Rev. B **85**, 045445 (2012).
[12] H.-Z. Lu, A. Zhao, and S.-Q. Shen, Phys. Rev. Lett. **111**, 146802 (2013).
[13] J. Kim, S.-H. Jhi, and R. Wu, Nano Lett. **16**, 6656 (2016).
[14] J.-M. Zhang, W. Ming, Z. Huang, G.-B. Liu, X. Kou, Y. Fan, K. L. Wang, and Y. Yao, Phys. Rev. B **88**, 235131 (2013).
[15] S. Qi, et al., Phys. Rev. Lett. **117**, 056804 (2016).
[16] W. Li, et al., Sci. Rep. **6**, 32732 (2016).
[17] A. M. Shikin, A. A. Rybkina, I. I. Klimovskikh, M. V. Filianina, K. A. Kokh, O. E. Tereshchenko, P. N. Skirdkov, K. A. Zvezdin, and A. K. Zvezdin, Appl. Phys. Lett. **109**, 222404 (2016).
[18] S. Grauer, K. M. Fijalkowski, S. Schreyeck, M. Winnerlein, K. Brunner, R. Thomale, C. Gould, and L. W. Molenkamp, Phys. Rev. Lett. **118**, 246801 (2017).
[19] C.-Z. Chang, W. Zhao, J. Li, J. K. Jain, C. Liu, J. S. Moodera, and M. H. W. Chan, Phys. Rev. Lett. **117**, 126802 (2016).
[20] P. E. Blöchl, Phys. Rev. B **50**, 17953 (1994).
[21] G. Kresse and D. Joubert, Phys. Rev. B **59**, 1758 (1999).
[22] G. Kresse and J. Hafner, Phys. Rev. B **49**, 14251 (1994).
[23] J. P. Perdew, K. Burke, and M. Ernzerhof, Phys. Rev. Lett. **77**, 3865 (1996).
[24] A. Tkatchenko and M. Scheffler, Phys. Rev. Lett. **102**, 073005 (2009).
[25] H. R. Fuh, K. W. Chang, S. H. Hung, and H. T. Jeng, IEEE Magn. Lett. **8**, 1 (2017).
[26] J. Liu, S. Y. Park, K. F. Garrity, and D. Vanderbilt, Phys. Rev. Lett. **117**, 257201 (2016).
[27] C.-J. Kang, H. C. Choi, K. Kim, and B. I. Min, Phys. Rev. Lett. **114**, 166404 (2015).
[28] D. J. Thouless, M. Kohmoto, M. P. Nightingale, and M. den Nijs, Phys. Rev. Lett. **49**, 405 (1982).
[29] Y. Yao, L. Kleinman, A. H. MacDonald, J. Sinova, T. Jungwirth, D.-s. Wang, E. Wang, and Q. Niu, Phys. Rev. Lett. **92**, 037204 (2004).
[30] A. A. Mostofi, J. R. Yates, Y.-S. Lee, I. Souza, D. Vanderbilt, and N. Marzari, Comput. Phys. Commun. **178**, 685 (2008).
[31] M. P. L. Sancho, J. M. L. Sancho, J. M. L. Sancho, and J. Rubio, J. Phys. F: Met. Phys. **15**, 851 (1985).
[32] See Supplemental Material at [URL] for the U effect and the thickness effect on the

electronic structure in V-doped Sb_2Te_3.
[33] J. Kim, S.-H. Jhi, A. H. MacDonald, and R. Wu, Phys. Rev. B **96**, 140410 (2017).
[34] J. Kim and S.-H. Jhi, Phys. Rev. B **92**, 104405 (2015).
[35] R. Yoshimi, K. Yasuda, A. Tsukazaki, K. S. Takahashi, N. Nagaosa, M. Kawasaki, and Y. Tokura, Nat. Commun. **6**, 8530 (2015).
[36] L. Vaugier, H. Jiang, and S. Biermann, Phys. Rev. B **86**, 165105 (2012).
[37] E. Şaşıoğlu, C. Friedrich, and S. Blügel, Phys. Rev. B **83**, 121101 (2011).
[38] S. Kim, K. Kim, C.-J. Kang, and B. I. Min, Phys. Rev. B **87**, 195106 (2013).